ANTIMICROBIAL AGENTS AND CHEMOTHERAPY, May 2006, p. 1828–1834 Vol. 50, No. 5
0066-4804/06/$08.00+0 doi:10.1128/AAC.50.5.1828–1834.2006

Photoinactivation of Mycobacteria In Vitro and in a New Murine Model of Localized *Mycobacterium bovis* BCG-Induced Granulomatous Infection

Katie O'Riordan,[1] David S. Sharlin,[1]† Jerome, Gross,[2] Sung Chang,[1] Divya Errabelli,[1]‡ Oleg E. Akilov,[1] Sachiko Kosaka,[1] Gerard J. Nau,[3]§ and Tayyaba Hasan[1]*

Wellman Center for Photomedicine, Massachusetts General Hospital and Harvard Medical School, Boston, Massachusetts[1]; Cutaneous Biology Research Center, Massachusetts General Hospital and Harvard Medical School, Charlestown Navy Yard, Charlestown, Massachusetts[2]; and Division of Infectious Diseases, Department of Medicine, Massachusetts General Hospital, Boston, Massachusetts[3]

Received 19 December 2005/Returned for modification 26 January 2006/Accepted 22 February 2006

Treatment of tuberculosis is currently hindered by prolonged antibiotic regimens and the emergence of significant drug resistance. Alternatives and adjuncts to standard antimycobacterial agents are needed. We propose that a direct attack utilizing photosensitizers and light-based treatments may be effective in curtailing *Mycobacterium tuberculosis* in discrete anatomical sites in the most infectious phase of pulmonary tuberculosis. To demonstrate experimental proof of principle, we have applied established photodynamic therapy (PDT) technology to in vitro cultures and an in vivo mouse model using *Mycobacterium bovis* BCG. We report here in vitro and in vivo PDT efficacy studies and the use of a three-dimensional collagen gel as a delivery vehicle for BCG, subcutaneously inserted, to induce specifically localized granuloma-like lesions in mice. When a benzoporphyrin derivative was utilized as the photosensitive agent, exposure to light killed extracellular and intracellular BCG in significant numbers. Collagen scaffolds containing BCG inserted in situ in BALB/c mice for 3 months mimicked granulomatous lesions and demonstrated a marked cellular infiltration upon histological examination, with evidence of caseating necrosis and fibrous capsule formation. When 10^5 BCG were present in the in vivo-induced granulomas, a significant reduction in viable mycobacterial cells was demonstrated in PDT-treated granulomas compared to those of controls. We conclude that PDT has potential in the treatment of localized mycobacterial infections, such as pulmonary granulomas and cavities.

Tuberculosis is a major public health problem worldwide and manifests as latent infection or progressive contagious disease (8). It has been estimated that one-third of the world's population is infected with *Mycobacterium tuberculosis*. The predominance of these infected cases is in the latent form; the remainder is active and often contagious. Although only 10% of infected people develop active tuberculosis (3), the death rate of about 2 million a year is among the highest for infectious diseases worldwide.

Current chemotherapeutic regimens, which are the mainstay in medical treatment for this recalcitrant pathogen, are losing effectiveness because of increasing bacterial resistance. Management of drug-resistant tuberculosis involves long-term, stringently monitored application of toxic second-line antibiotics (15, 20) and sometimes surgical resection, each of which can be associated with high morbidity (7, 27). Currently, there exists a substantial research effort to develop effective vaccines (1, 5, 14, 30).

The pathology of active, secondary pulmonary tuberculosis in adults is mostly limited to the upper lobes, where the mycobacteria are contained within a few large, caseating granulomas (18). This localization, which happens to be associated with the highest level of infectivity, encourages the development of a treatment, such as photodynamic therapy (PDT), aimed at directly killing the bacteria. Photodynamic therapy is a photochemistry-based modality in which localized light-activated molecules produce cytotoxic molecular species (2, 12). The potential of PDT in targeting infectious pathogens has been reviewed recently (10, 16, 23).

We report here the development of a convenient localized model of granulomatous infection, and we examined the efficacy of PDT using a benzoporphyrin derivative (BPD-PDT) to kill mycobacteria in culture and using this in vivo model. We propose that PDT, with its localized phototoxic property, reported effectiveness against drug-resistant pathogens, and use in treating certain cancers of the lung (22), could play an important role in the treatment of pulmonary granulomas in persons with active disease and in drug-resistant infections by significantly reducing the microbial burden.

* Corresponding author. Mailing address: Wellman Center for Photomedicine, Massachusetts General Hospital, BAR 314, 40 Blossom Street, Boston, MA 02114. Phone: (617) 726-6996. Fax: (617) 726-8566. E-mail: thasan@partners.org.

† Present address: Molecular and Cellular Biology Program, University of Massachusetts, Amherst, MA 01003.

‡ Present address: Center for Human Genetics, Boston University, Boston, MA 02118.

§ Present address: Departments of Molecular Genetics and Biochemistry and Medicine, University of Pittsburgh School of Medicine, Pittsburgh, Pa.

MATERIALS AND METHODS

Bacterial strains and culture conditions. *Mycobacterium bovis* bacillus Calmette-Guérin (BCG) strain Pasteur was obtained from the ATCC (ATCC

35734; Trudeau mycobacterial culture collection 1011 "BCG Pasteur"). A BCG strain expressing firefly luciferase (rBCG-lux) was a gift from Kendall Stover (PathoGenesis Inc., Seattle, Wash.) (13) and was used for all in vivo studies. Strains were cultured in Difco Middlebrook 7H9 broth (BD, Sparks, MD) containing Middlebrook albumin, dextrose, and catalase enrichment at 37°C with constant agitation, using a magnetic stirrer to prevent excessive clumping of cells. For determination of numbers of CFU, 7H10 agar plates containing Middlebrook albumin, dextrose, catalase, and, to prevent fungal growth, cycloheximide (200 μg/ml) were used. All plates were incubated at 37°C in the presence of 5% CO_2 for 2 to 3 weeks. During culturing of rBCG-lux, kanamycin (20 μg/ml) was incorporated into broth and agar. When intracellular growth was required, bacteria were cocultured with J774.2 cells (ATCC, Rockville, MD), using a ratio of infection of 5 to 10 bacteria per macrophage, in RPMI 1640 (Mediatech, Herndon, VA) with 10% heat-inactivated fetal calf serum.

Radiolabeled uracil uptake assay. In vitro measurements of BCG viability were also performed by using a [^{3}H]uracil assay as previously described (21).

Photosensitizer. Verteporfin (lipid-formulated benzoporphyrin derivative monoacid ring A) was obtained from QLT Inc. (Vancouver, Canada). A stock saline solution of verteporfin was reconstituted according to the manufacturer's instructions and stored at 4°C in the dark.

Preparation of sterile and bacterial populated collagen scaffolds. Purified bovine tendon collagen (dissolved in cold 0.1 M acetic acid at a concentration between 0.1 and 0.2%) was a gift from Organogenesis Inc. (Canton, MA). For preparation of collagen scaffolds for implantation, cold-purified dissolved collagen, RPMI 1640, fetal calf serum, sodium chloride, sodium bicarbonate, and, when required, BCG cells were mixed in a 1.5-ml tube and allowed to polymerize at 37°C overnight. The resultant soft gels were centrifuged (10,000 × *g* for 10 min) to obtain compact pellets that could be conveniently placed in the mouse. During the preparation of mycobacteria for inclusion into the collagen scaffolds, it was necessary to sonicate (three 20-s bursts) the normally aggregating bacteria in a Fisher Scientific sonic dismembrator model 100, using a cup horn attachment to ensure relatively uniform cell dispersions. The optical density of the culture at 600 nm was then measured and adjusted by diluting the culture in 7H9 medium to allow the required numbers of BCG in a 10-μl volume.

Mouse model of localized infection, recovery, and assay of mycobacteria from implanted scaffolds. Male BALB/c mice (6 to 8 weeks old, 20 to 25 g) obtained from Charles River Laboratories (Wilmington, MA) were used throughout the study. All animal procedures were performed according to protocols approved by the Massachusetts Hospital Subcommittee on Research Animal Care. Mice were anesthetized with an intraperitoneal injection of ketamine (90 mg/kg of body weight) and xylazine (10 mg/kg). One full-thickness incisional skin wound was made in a line along the dorsal surface, and a subcutaneous pocket was made with fine-tipped sterile forceps. The collagen implants were placed at either side of the dorsal midline, and the incisions were then closed with two or three 4.0 nylon sutures. Following humane sacrifice of the animals, the residual implants were recovered and digested with 5% collagenase (type I from *Clostridium histolyticum*; Sigma, St. Louis, MO) for 1 hour at 37°C. The digested mixture was then sonicated briefly using a cup horn sonicator, and dilutions were prepared in 7H9 broth. Enumeration of viable bacteria was performed by CFU determination or by radiolabeled uracil uptake analysis.

In vivo fluorescence imaging. As BPD is fluorescent, this quality was exploited to quantitate the amount delivered to the collagen implant. Relative concentration of BPD delivered to the collagen implants in the mouse model was quantified using an in vivo fluorescence microscope, consisting of a blue LED light source (Luxeon LXHL-MRRC; Lumileds Lighting, San Jose, CA) coupled to an exciter filter (HQ455/70; Chroma Technology, Rockingham, VT), a long-working-distance objective with 10× magnification (Mitutoyo M Plan Apo 10×; Mitutoyo, Aurora, IL), and a high-sensitivity charge-coupled-device camera (Cascade 512F; Photometrics, Tucson, AZ) with an emitter filter (HQ700/75; Chroma Technology, Rockingham, VT). Each image was acquired with a 2-mm by 2-mm field of view and a 200-ms exposure time. In order to account for variations in light source intensity and camera sensitivity, a positive standard consisting of 0.01 M LDS laser dye (Exciton, Dayton, OH) in a quartz cuvette was measured daily, and all reported fluorescence intensities from the microscope images were normalized using this standard. Nonpopulated collagen scaffolds were implanted in the dorsal skin of mice for up to 4 weeks. After anesthesia and BPD injection (1 mg/kg), the collagen implant was exposed by excising the dorsal skin and was imaged every 10 to 20 min for up to 60 min using the fluorescence microsope. The relative concentration of BPD, quantified from the fluorescence images, was validated by measuring BPD fluorescence using a spectrofluorometer, and the presence of an emission peak at 690 nm confirmed the presence of BPD. Each collagen implant was harvested and collagenase digested, and its fluorescence spectrum (450-nm excitation) was measured using a SPEX FluoroMax 3 spectrofluorometer (Jobin Yvon, Edison, NJ). In order to account for the fluorescence from the collagenase-digested collagen, the fluorescence spectra of appropriate controls (450-nm excitation) were measured and subtracted from the sample measurements. A titration curve to quantify BPD concentration from the fluorescence images was derived using collagen scaffolds mixed with different concentrations of BPD (0.1 μg to 2.5 μg) that were imaged using the fluorescence microscope, and the fluorescence spectra were measured with the fluorometer after collagenase digestion.

TABLE 1. Effect of PDT on extracellular and intracellular *M. bovis* BCG (Pasteur)[a]

Treatment of BCG cells	% Survival after treatment (mean ± SE)
BPD only	87.0 ± 12.3
Light only	104.0 ± 4.9
BPD and light	26.0 ± 14.4**
BPD and light in J774 monolayer	49.0 ± 22.0

[a] Survival of BCG cells following exposure to BPD only (5 μM BPD for 1 h), light only (60 J/cm^2 of 690-nm light), and both BPD and light (5 μM BPD for 1 h and 60 J/cm^2 of 690-nm light). Survival is expressed as a percentage of the control ± standard error. Control samples (set to 100%) contained 2×10^8 bacteria/ml of log-phase cells. Values represent means from four independent experiments. For survival of BCG cells in a J774 monolayer, PDT-treated samples were expressed as percentages of control BCG cells in a J774 monolayer (100%), and the value represents the mean from three independent experiments ± standard error. Viability in all experiments was determined using the radiolabeled uracil uptake assay. **, $P < 0.01$.

PDT treatment. A diode laser system (HPD Inc., North Brunswick, NJ) with a 690-nm wavelength was used throughout this study. The light was delivered through an optical fiber using a fiber optic collimator. For in vitro studies, cells were incubated with 5 μM BPD for 1 hour in the dark and then transferred to 35-mm petri dishes and exposed to the light source at fluences of 60 to 100 J/cm^2. Following irradiation, cells were resuspended in fresh medium for 12 h, and then viability was determined by colony formation or the radiolabeled uracil uptake assay. For in vivo studies, animals were anesthetized with an intraperitoneal injection of ketamine (90 mg/kg) and xylazine (10 mg/kg) and placed on a heating pad, maintained at 37°C throughout the treatments. Photosensitizer (BPD) was administered intravenously (0.5 mg/kg) and allowed to circulate for 1 hour, and then the site of the subcutaneous implant was typically exposed transcutaneously to a fluence rate of 65 mW/cm^2 for 920 seconds (60 J/cm^2), as measured by a LaserMate power meter (Coherent Inc., Santa Clara, CA).

Histology. Excised artificial granulomas were fixed in 10% neutral formalin, paraffin embedded, and then stained with hematoxylin and eosin (H&E) or Ziehl-Neelsen stain for acid-fast bacteria.

Statistical analysis. The statistical analysis was based on the calculation of the arithmetic mean and standard error. The difference between two means was compared by a two-tailed, unpaired Student *t* test. A *P* value of less than 0.05 was considered statistically significant.

RESULTS

Antimycobacterial activity of BPD-PDT in vitro. Preliminary studies identified conditions of 5 μM BPD and fluences between 60 J/cm^2 and 100 J/cm^2 of 690-nm light as optimal for antimycobacterial activity for the photosensitizer BPD. These parameters were used for the in vitro experiments whose results are presented in Table 1. Under these conditions, only 26% of *M. bovis* BCG (Pasteur) cells remained viable after PDT, with numbers decreasing from 2×10^8 to 4×10^7 CFU (Table 1), although 87% of mycobacterial cells treated with BPD only (no light activation) survived and cells irradiated with 690-nm light, without BPD, demonstrated 104% survival compared to untreated cells (Table 1). Bacteria associated with J774 cells were modestly more resistant to the effects of BPD. Under the same conditions used for extracellular bacteria, on average 50% of the BCG were killed by BPD-PDT when they

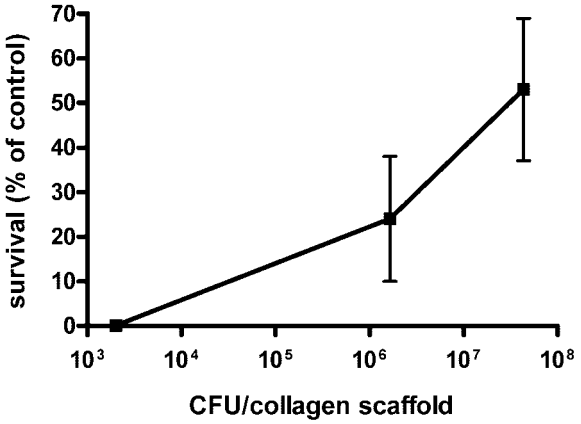

FIG. 1. Effect of microbial burden in collagen scaffolds on efficacy of PDT in vitro. Survival of rBCG-lux in a collagen scaffold after treatment with 5 μM BPD for 1 h and irradiation with 100 J/cm^2 of 690-nm light compared to that of untreated cells. Viability was determined by the number of CFU on 7H10 agar containing kanamycin. Mean values ± standard errors are represented.

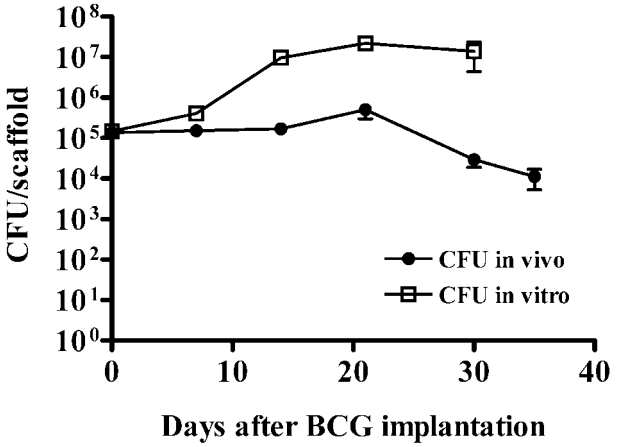

FIG. 2. Time course of BCG infection in collagen scaffolds implanted in BALB/c (*Nramp1*^{s}) mice and in vitro at 37°C. At day 0, mice were implanted with collagen scaffolds containing 10^5 BCG cells. At indicated time points, animals were sacrificed and numbers of viable mycobacteria in collagen scaffolds enumerated by CFU determination on agar plates. Data represent the means ± standard errors (n = 24 mice).

were cocultured with J774 cells (Table 1). The reduced killing effect observed for intracellular BCG was most likely due to a comparatively diminished interaction between BPD and the bacterial cells. However, J774 cells accumulated photosensitizer and were destroyed upon PDT, and this mechanism of BPD-PDT killing may influence BCG viability, as many reports indicate that mycobacteria may be killed when macrophages undergo tumor necrosis factor- or Fas-mediated apoptosis, whereas necrosis does not appear to affect viability (24, 26).

We next tested whether the BPD-PDT strategy would be effective in a more complex culture environment, such as the BCG-populated collagen gel used for in vivo studies. Despite the increased complexity, BPD-PDT was phototoxic against BCG in vitro when cells were incubated with 5 μM BPD for 1 h prior to irradiation with a 690-nm diode laser (fluence, 100 J/cm^2; fluence rate, 40 mW/cm^2). At low bacterial density (10^3 rBCG-lux per scaffold), no surviving mycobacterial cells could be detected upon plating and incubation of the entire digested collagen gel (Fig. 1). This suggested that BPD was capable of permeating the entire scaffold, reaching bacteria harbored in the center of the structure, which was confirmed by confocal microscopy (data not shown). Under these experimental conditions (fluence, 100 J/cm^2; fluence rate, 40 mW/cm^2), it was observed that as the microbial burden increased to 10^6 or 10^7 BCG, the killing efficiency decreased, with 50% killing observed when 4×10^7 bacteria were present per scaffold (Fig. 1).

Development of a model of localized *M. bovis* BCG infection in BALB/c mice using collagen scaffolds. The behavior of BCG-populated collagen implants was examined in vivo. In vivo bioluminescence imaging, as previously described (11), was evaluated as a tool to monitor *M. bovis* rBCG-lux numbers in BALB/c mice over time. Though this method was convenient for detecting more than 10^8 rBCG-lux cells, it lacked sensitivity in detecting less that 10^5 cells per collagen implant (data not shown). Therefore, enumeration by CFU determination was always used either alone or in conjunction with this luminescence imaging. Over the first 21 days after implantation of 10^5 *M. bovis* rBCG-lux-populated scaffolds in BALB/c mice, there was a modest increase in cell numbers (less than 1 $\log_{10}$), which subsequently declined over the following 10 days to 10^4 bacteria/implant (Fig. 2). Growth of rBCG-lux in vitro at 37°C in similarly prepared scaffolds demonstrated an exponential increase in cell numbers over 14 days and then a plateau (Fig. 2). This experiment suggests that the declining pattern was unique to the local in vivo immune environment and not due to any inherent inhibitory properties of the collagen. The typical positioning and appearance of the implants in the mouse are indicated in Fig. 3. The implants were grossly visible externally on the dorsal region of the mouse (Fig. 3A). They were usually

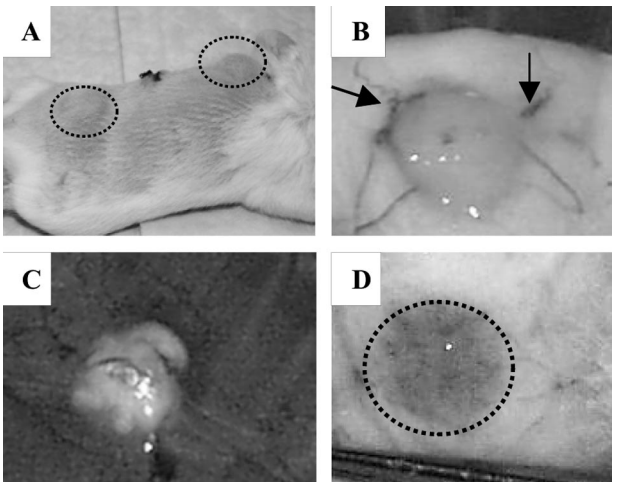

FIG. 3. Gross appearance of collagen scaffolds containing *M. bovis* BCG in BALB/c mice. (A) Gross macroscopic appearance of mouse with subcutaneous implants 1 week after implantation (circled areas). (B) The skin flap reveals the implant adhering to the underside of the skin, and arrows denote vessels surrounding the pellet that were typically observed as early as 1 week postimplantation. (C) Implants in situ for 3 months revealed possible caseous necrosis. (D) Vascular footprint (circle) that remains after removal of gel implant.

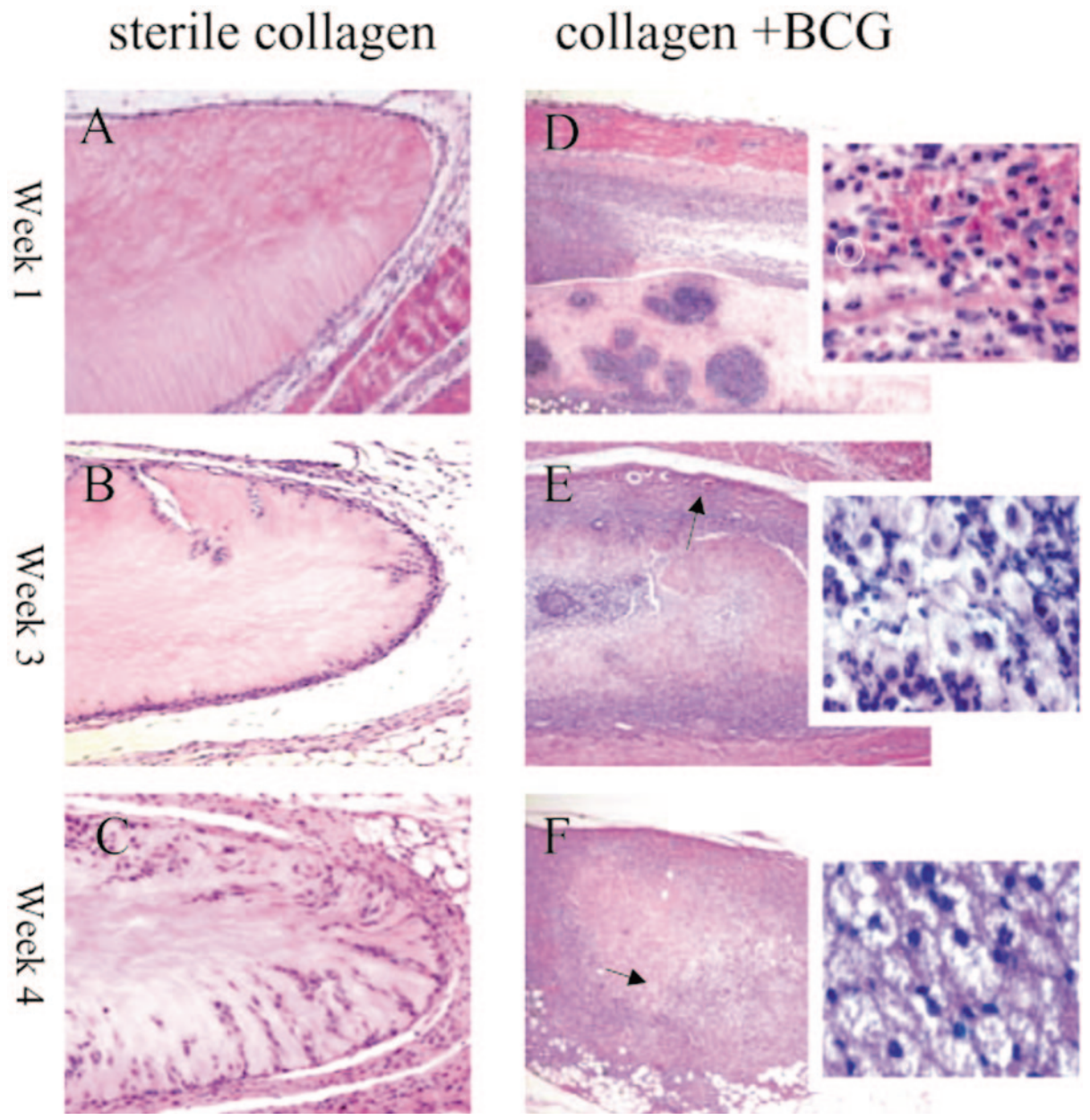

FIG. 4. Histological sectioning (H&E staining) of collagen scaffolds implanted subcutaneously in mice for 1, 3, and 4 weeks. Panels A to C (magnification, ×100) represent implanted collagen scaffolds that did not contain *M. bovis* BCG that were in situ for 1 week (A), 3 weeks (B), and 4 weeks (C). Little cellular recruitment into the collagen scaffolds was observed compared to that shown in panels D to F (magnification, ×50) with their respective insets (magnification, ×630 using water immersion objective), which represent BCG-containing scaffolds that were implanted for 1, 3, and 4 weeks, respectively. Massive cellular recruitment is marked by the abundance of hematoxylin-stained nuclei throughout the gel (D to F). After 1 week (D), mononuclear cells predominated (typical neutrophil circled), whereas at 3 weeks (E) and 4 weeks (F), macrophages became the dominant cell population and possible lymphocytes began to appear. Vascularization of the fibrous capsule was evident from week 3 (arrow in panel E). After 4 weeks, an eosinophilic acellular pattern was observed in the infected scaffolds (arrow in panel F). A lower magnification was used for BCG-containing scaffolds to capture the full extent of inflammation, and a higher magnification was used to reveal individual cell types of the infiltrate.

adherent to the overlying subcutaneous tissue and not the underlying fascia (Fig. 3B). Vasculature was often observed associated with the implants as early as 1 week postimplantation (Fig. 3B). After 3 months in situ, the implants were friable and had degenerated to a soft, cheese-like texture (Fig. 3C). These findings are consistent with an interpretation of caseous necrosis. Robust vascular footprints were typically visible upon removal of the implants (Fig. 3D).

Dramatic histologic differences were observed between implanted infected and sterile collagen scaffolds (Fig. 4). Cellular recruitment into the sterile collagen scaffolds was delayed until week 4 after implantation, and the infiltrate was considerably

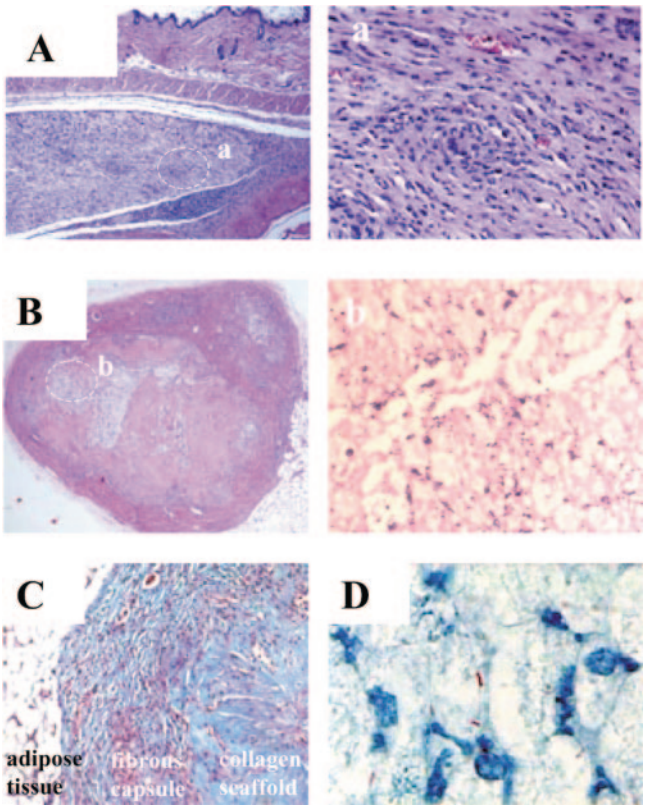

FIG. 5. Histological sectioning of collagen scaffolds that remained in situ for 3 weeks or 3 months. (A) At 3 weeks, granulomatous foci were visible (magnification, ×50) which upon higher magnification in panel a (magnification, ×200), revealed concentric arrangements of host cell infiltrates. Panel B (magnification, ×50) represents an H&E-stained section of a scaffold implanted for 3 months in which the scaffold is encapsulated by a dense layer of newly formed collagen. There appears to be evidence of necrosis toward the center of the granuloma, which can be more clearly observed at a higher magnification (magnification, ×400) (b). (C) A trichrome stain performed to confirm the presence of the fibrous capsule at 3 months (magnification, ×100). A deposited layer of dense fibrotic material (stained dark blue) surrounding the implanted scaffold was observed. The collagenous matrix of the scaffold stained a paler shade of blue. Panel D represents a Ziehl-Neelsen stain (magnification, ×1,000) where the red acid-fast bacteria could be visualized and appeared to be well associated with the large, foamy, macrophage-like host cell infiltration.

less than that observed in the BCG-populated scaffolds, which were composed predominantly of macrophages (Fig. 4A to C). The appearance of cellular recruitment and fibrous capsule formation in the sterile scaffolds was typical for a mild foreign body-type immune response. In contrast, the collagen scaffold populated with 10^5 BCG revealed tuberculous granuloma-like formation. After the first week in situ (Fig. 4D and inset), a marked cellular recruitment of mononuclear cells, possibly neutrophils (typical neutrophil circled in insert), and some macrophages were observed in the infected scaffolds. Vascularization of the fibrous capsule was observed during week 3, likely promoting further recruitment of immune cells toward the infectious granuloma (Fig. 4E). At week 3, the infiltrate was composed of a mixed population, probably consisting of macrophages and neutrophils (Fig. 4E inset). After 4 weeks, the implants showed amorphous, eosinophilic, acellular debris (Fig. 4F). Intense mononuclear cellular infiltration was present (Fig. 4F inset), and putative lymphocytes began to appear. The granulomatous foci observed at 3 weeks (Fig. 5A) revealed at higher magnifications concentric arrangements of macrophages (Fig. 5a). Comparative examination of implants that remained in situ in BALB/c mice for 3 months revealed even more dramatic changes. Massive cellular infiltration observed at 3 months (Fig. 5B) displayed extensive areas of necrosis (Fig. 5b). The presence of a fibrous capsule at 3 months was tentatively identified by trichrome staining (Fig. 5C), in which the dense fibrotic material surrounding the capsule stained dark blue. Acid-fast staining of implants confirmed the presence of BCG associated with the cellular infiltration (Fig. 5D).

In vivo imaging of photosensitizer delivery to subcutaneous collagen scaffolds. In vivo fluorescence analysis was performed first to determine whether the intravenous-administered photosensitizer penetrated the subcutaneous implants. Mice injected with 1 mg/kg BPD (the therapeutic dose of 0.5 mg/kg was below our detection limits) were imaged in vivo for photosensitizer fluorescence. Fluorescence images of control in vitro collagen scaffolds mixed with known amounts of BPD indicated that fluorescence intensity increases linearly between 0.1 μg and 2.5 μg of BPD (Fig. 6A). A titration curve to convert fluorescence intensity to BPD concentration was formulated based on this observation. The delivery of BPD to the collagen implants was observed in vivo from the fluorescence microscopy images, and that the fluorescence was due to the presence of BPD in the collagen was confirmed by verifying the presence of a typical fluorescence peak (690 nm) using a spectrofluorometer. Figure 6B (i to iii) shows typical BPD fluorescence images of a collagen scaffold implanted subcutaneously for 4 weeks. Fluorescence intensity increased linearly immediately after BPD injection up to 60 min, suggesting steady, time-dependent delivery of BPD to the collagen implants. Based on the titration curve, the fluorescence images indicate that approximately 1 μg BPD was delivered to the collagen pellet implanted for 4 weeks.

Antimycobacterial activity of PDT in vivo. Compared with untreated control granulomas, 26% of BCG survived in PDT-treated, in vivo-induced granulomas initially containing approximately 10^5 BCG (Fig. 7). This corresponded to a 0.7-$\log_{10}$ reduction in viable bacterial cell counts and thus was similar to results obtained in vitro for a comparable microbial burden.

DISCUSSION

In 1900, Niels Finsen was awarded the Nobel Prize for his invention of light therapy for skin tuberculosis, and the underlying mechanism for this successful therapy has been proposed to be excitation of endogenous porphyrins in *M. tuberculosis* (19). We report here a fresh effort to determine whether the application of photodynamic therapy applied to experimentally localized mycobacteria can be developed as a new effective tool alongside chemotherapeutics in the fight against tuberculosis. We demonstrated significant in vitro killing of *M. bovis* BCG both extra- and intracellularly and when incorporated into a collagen scaffold. The effectiveness of the PDT killing action within the collagen scaffolds was linked to the microbial burden present. As the microbial burden of the scaffolds increased, the PDT killing effect was reduced (Fig. 1). The in-

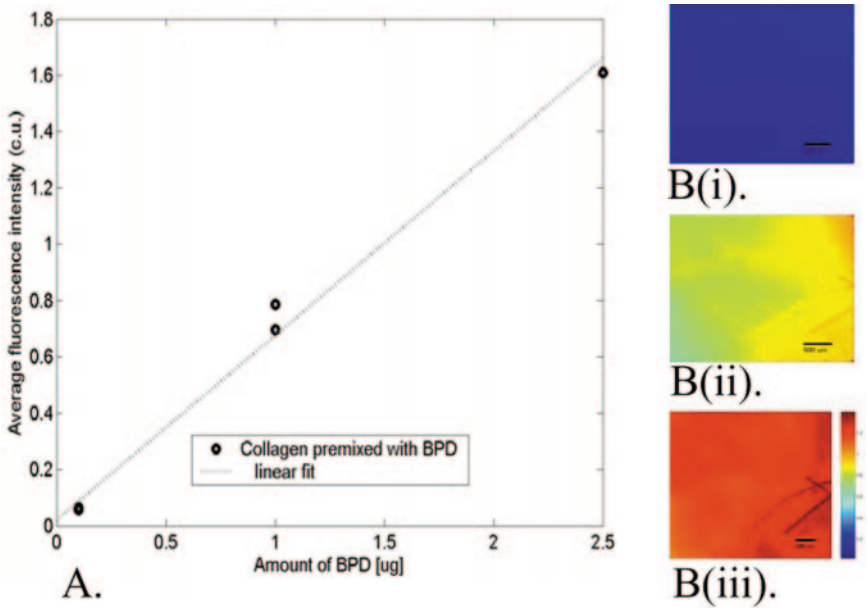

FIG. 6. (A) Correlation of the calibrated fluorescence intensity (calibrated units [c.u.]) from the in vivo fluorescence microscopy images with the amount of BPD mixed into the collagen pellets. Four different samples were mixed with either 0 mg, 0.1 mg, 1.0 mg, or 2.5 mg BPD. The average calibrated intensity from the fluorescence microscopy images of each pellet is plotted with the amount of BPD added to each pellet. (B) Typical calibrated fluorescence images acquired from collagen implants (i) before BPD injection, (ii) 30 min after BPD injection, and (iii) 60 min after BPD injection. An identical brightness scale was employed for all the images, as shown in panel B(iii).

fluence of cell density on the success of photoinactivation of *Escherichia coli* and *Staphylococcus aureus* has recently been reported by others, who proposed that competition for binding sites at higher cell densities results in reduced photosensitizer bound per cell (4). It is possible in the case of mycobacteria that the marked tendency of these bacteria to aggregate further masks sites required for photosensitizer association with the cell. Approaches for increasing photosensitizer concentration are under study, as is the search for increasingly effective photosensitizers.

Although it is widely accepted that the guinea pig is one of the more appropriate models for investigating aspects of *Mycobacterium* infection due to its ability to form necrotic lung granulomas (28), the mouse is the most frequently utilized model. However, the loosely organized murine granuloma structures and high persisting bacterial population do not reproduce many of the critical features of the human condition (6). With our collagen scaffold implantation model, we sought to establish a localized infection that would induce a more highly organized granulomatous response. In addition, the bacteria and the induced granuloma are readily recoverable for further analysis. Purified minimally immunogenic collagen permits control over constituents of the scaffold compared to more-heterogenous matrices, such as Matrigel, recently employed by others (25).

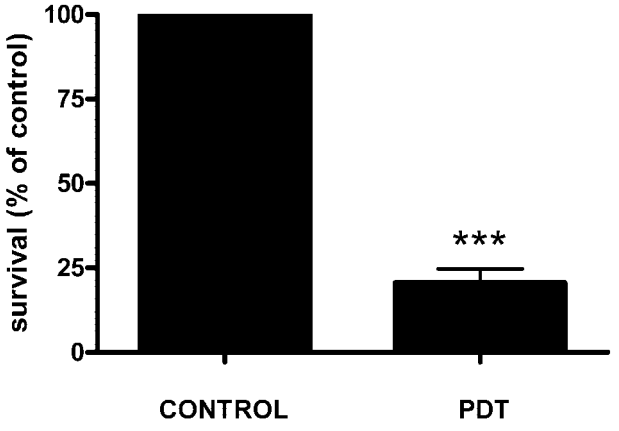

FIG. 7. Antimycobacterial effect of PDT on induced granulomas in BALB/c mice. Collagen scaffolds were implanted in mice for 3 weeks, after which mice received 0.5 mg/kg BPD, and after 1 hour, they were irradiated with 60 J/cm^2 of 690-nm light (fluence rate, 65 mW/cm^2). Bacterial viability was assessed 72 h after a single treatment by determining numbers of CFU on Middlebrook agar (***, $P < 0.001$).

The BALB/c strain of mice was chosen for our initial studies due to their *Nramp1*^{s} genotype (17). Prone to a Th2 immune response, these mice are susceptible to granulomatous diseases (31). The progression of BCG growth in our collagen scaffolds in vivo parallels well with observations of various organs in BALB/c mice reported by others (9, 17, 29). An initial increase in BCG numbers was followed by a decline of more than 1 log and subsequent persistence. A different in vitro growth pattern indicated that this did not reflect some condition unique to the collagen but rather is dependent on the in vivo local immune environment. Histological analysis indicated that the lesions did share many features with pulmonary tuberculous granulomas; pronounced cellular infiltration occurs in BCG-populated collagen implants. At 3 months, the formation of a fibrous capsule in the control implants could be observed, and there was evidence of caseous necrosis. Such pathological features are rarely observed in other mouse models.

PDT of subcutaneous BCG-containing granulomas yielded

antimicrobial activity similar to that detected from in vitro experiments, with a 0.7-$\log_{10}$ decrease in cell numbers observed when 10^5 BCG were present. This 80% reduction in viable bacterial numbers after a single therapy is significant, and future studies in this laboratory will determine whether multiple activations using BPD can achieve a sterilization effect. A plethora of other photosensitizers exists, some of which are likely to be even more inhibitory to *Mycobacterium*.

In summary, this represents the first comprehensive report of photochemical killing of mycobacteria. The long-term goal of this work is to evaluate the application of PDT not only for cutaneous mycobacterial diseases but, more significantly, for localized pulmonary sites, such as granulomas and cavities. Future studies in our laboratory will evaluate the formation of granulomas in guinea pig lung using the same collagen scaffold technology. We will investigate the antimycobacterial activity of PDT using this modified model. The application of PDT to pulmonary sites, although challenging, has already been achieved in the clinics for certain indications of non-small-cell lung carcinomas (information available at http://www.fda.gov). More recently, peripheral lung tumors have been treated using percutaneous fiber optics for light delivery (22). These applications could be reasonably adapted for the treatment of localized pulmonary granulomas. The findings presented in this study demonstrate proof of principle sufficient to warrant more investigation both to optimize the methodologies and to prove their applicability to effective treatment of localized pulmonary tuberculosis.

ACKNOWLEDGMENTS

This work was funded by Department of Defense Medical Free Electron Laser Program grant no. FA9550-04-1-0079 and by the Mattina Proctor Foundation. Current support (for J. Gross) comes from the Cutaneous Biology Research Center through the MGH Shiseido Co. Ltd. Agreement.

We thank QLT (Vancouver, Canada) for the generous gift of BPD (verteporfin) and Organogenesis Inc. (Canton, MA) for bovine collagen.

REFERENCES

1. **Andersen, P., and T. M. Doherty.** 2005. The success and failure of BCG–implications for a novel tuberculosis vaccine. Nat. Rev. Microbiol. **3:**656–662.
2. **Castano, A. P., T. N. Demidova, and M. R. Hamblin.** 2004. Mechanisms in photodynamic therapy. I. Photosensitizers, photochemistry and cellular localization. Photodiagn. Photodynam. Ther. **1:**279–293.
3. **Chan, J., and J. Flynn.** 2004. The immunological aspects of latency in tuberculosis. Clin. Immunol. **110:**2–12.
4. **Demidova, T. N., and M. R. Hamblin.** 2005. Effect of cell-photosensitizer binding and cell density on microbial photoinactivation. Antimicrob. Agents Chemother. **49:**2329–2335.
5. **Doherty, T. M., and P. Andersen.** 2005. Vaccines for tuberculosis: novel concepts and recent progress. Clin. Microbiol. Rev. **18:**687–702.
6. **Duncan, K., and C. E. Barry III.** 2004. Prospects for new antitubercular drugs. Curr. Opin. Microbiol. **7:**460–465.
7. **Freixinet, J. G., J. J. Rivas, F. Rodriguez De Castro, J. A. Caminero, P. Rodriguez, M. Serra, M. de la Torre, N. Santana, and E. Canalis.** 2002. Role of surgery in pulmonary tuberculosis. Med. Sci. Monit. **8:**CR782–CR786.
8. **Glickman, M. S., and W. R. Jacobs, Jr.** 2001. Microbial pathogenesis of *Mycobacterium tuberculosis*: dawn of a discipline. Cell **104:**477–485.
9. **Gros, P., E. Skamene, and A. Forget.** 1981. Genetic control of natural resistance to *Mycobacterium bovis* (BCG) in mice. J. Immunol. **127:**2417–2421.
10. **Hamblin, M. R., and T. Hasan.** 2004. Photodynamic therapy: a new antimicrobial approach to infectious disease? Photochem. Photobiol. Sci. **3:**436–450.
11. **Hamblin, M. R., T. Zahra, C. H. Contag, A. T. McManus, and T. Hasan.** 2003. Optical monitoring and treatment of potentially lethal wound infections in vivo. J. Infect. Dis. **187:**1717–1725.
12. **Hasan, T., B. Ortel, A. C. E. Moor, and B. W. Pogue.** 2003. Photodynamic therapy of cancer, p. 605–622. *In* D. Kute, R. Pollock, R. Weichselbaum, et al. (ed.), Cancer medicine. Decker Inc., Hamilton, Ontario, Canada.
13. **Hickey, M. J., T. M. Arain, R. M. Shawar, D. J. Humble, M. H. Langhorne, J. N. Morgenroth, and C. K. Stover.** 1996. Luciferase in vivo expression technology: use of recombinant mycobacterial reporter strains to evaluate antimycobacterial activity in mice. Antimicrob. Agents Chemother. **40:**400–407.
14. **Hoag, H.** 2004. New vaccines enter fray in fight against tuberculosis. Nat. Med. **10:**6.
15. **Iseman, M. D.** 1998. MDR-TB and the developing world–a problem no longer to be ignored: the WHO announces 'DOTS Plus' strategy. Int. J. Tuberc. Lung Dis. **2:**867.
16. **Jori, G., and S. B. Brown.** 2004. Photosensitized inactivation of microorganisms. Photochem. Photobiol. Sci. **3:**403–405.
17. **Mazzolla, R., M. Puliti, R. Barluzzi, R. Neglia, F. Bistoni, G. Barbolini, and E. Blasi.** 2002. Differential microbial clearance and immunoresponse of Balb/c (Nramp1 susceptible) and DBA2 (Nramp1 resistant) mice intracerebrally infected with *Mycobacterium bovis* BCG (BCG). FEMS Immunol. Med. Microbiol. **32:**149–158.
18. **McKinney, J. D., W. R. Jacobs, Jr., and B. R. Bloom.** 1998. Persisting problems in tuberculosis, p. 51–156. *In* R. M. Krause (ed.), Emerging infections. Academic Press, New York, N.Y.
19. **Moller, K. I., B. Kongshoj, P. A. Philipsen, V. O. Thomsen, and H. C. Wulf.** 2005. How Finsen's light cured lupus vulgaris. Photodermatol. Photoimmunol. Photomed. **21:**118–124.
20. **Nathanson, E., R. Gupta, P. Huamani, V. Leimane, A. D. Pasechnikov, T. E. Tupasi, K. Vink, E. Jaramillo, and M. A. Espinal.** 2004. Adverse events in the treatment of multidrug-resistant tuberculosis: results from the DOTS-Plus initiative. Int. J. Tuberc. Lung Dis. **8:**1382–1384.
21. **Nau, G. J., L. Liaw, G. L. Chupp, J. S. Berman, B. L. Hogan, and R. A. Young.** 1999. Attenuated host resistance against *Mycobacterium bovis* BCG infection in mice lacking osteopontin. Infect. Immun. **67:**4223–4230.
22. **Okunaka, T., H. Kato, H. Tsutsui, T. Ishizumi, S. Ichinose, and Y. Kuroiwa.** 2004. Photodynamic therapy for peripheral lung cancer. Lung Cancer **43:**77–82.
23. **O'Riordan, K., O. E. Akilov, and T. Hasan.** 2005. The potential for photodynamic therapy in the treatment of localized infections. Photodiagn. Photodynam. Ther. **2:**247–262.
24. **Park, J. S., M. H. Tamayo, M. Gonzalez-Juarrero, I. M. Orme, and D. J. Ordway.** 2006. Virulent clinical isolates of *Mycobacterium tuberculosis* grow rapidly and induce cellular necrosis but minimal apoptosis in murine macrophages. J. Leukoc. Biol. **79:**80–86.
25. **Rhoades, E. R., R. E. Geisel, B. A. Butcher, S. McDonough, and D. G. Russell.** 2005. Cell wall lipids from *Mycobacterium bovis* BCG are inflammatory when inoculated within a gel matrix: characterization of a new model of the granulomatous response to mycobacterial components. Tuberculosis (Edinburgh) **85:**159–176.
26. **Spira, A., J. D. Carroll, G. Liu, Z. Aziz, V. Shah, H. Kornfeld, and J. Keane.** 2003. Apoptosis genes in human alveolar macrophages infected with virulent or attenuated *Mycobacterium tuberculosis*: a pivotal role for tumor necrosis factor. Am. J. Respir. Cell Mol. Biol. **29:**545–551.
27. **Takeda, S., H. Maeda, M. Hayakawa, N. Sawabata, and R. Maekura.** 2005. Current surgical intervention for pulmonary tuberculosis. Ann. Thorac. Surg. **79:**959–963.
28. **Turner, O. C., R. J. Basaraba, and I. M. Orme.** 2003. Immunopathogenesis of pulmonary granulomas in the guinea pig after infection with *Mycobacterium tuberculosis*. Infect. Immun. **71:**864–871.
29. **Vidal, S. M., D. Malo, K. Vogan, E. Skamene, and P. Gros.** 1993. Natural resistance to infection with intracellular parasites: isolation of a candidate for BCG. Cell **73:**469–485.
30. **von Reyn, C. F.** 2005. Tuberculosis vaccine trials. Lancet Infect. Dis. **5:**132.
31. **Wells, C. A., T. Ravasi, G. J. Faulkner, P. Carninci, Y. Okazaki, Y. Hayashizaki, M. Sweet, B. J. Wainwright, and D. A. Hume.** 2003. Genetic control of the innate immune response. BMC Immunol. **4:**5.